Journal of Nuclear Materials 385 (2009) 299–303

Contents lists available at ScienceDirect

Journal of Nuclear Materials

journal homepage: www.elsevier.com/locate/jnucmat

Irradiation effects in helium implanted silicon carbide measured by X-ray absorption spectrometry

Manuel A. Pouchon [a,*], Jiachao Chen [a], Annick Froideval [a], Markus Janousch [b], Claude Degueldre [a]

[a] Paul Scherrer Institut, Nucl. Energy and Safety, 5232 Villigen PSI, Switzerland
[b] Paul Scherrer Institut, Swiss Light Source, 5232 Villigen PSI, Switzerland

ARTICLE INFO

PACS:
61.05.cj
81.05.Je
61.80.−x
28.41.Qb
28.50.Hw

ABSTRACT

Silicon carbide (SiC) is investigated as a possible structural material for future nuclear power plants. It is utilized as fibre and/or as matrix in ceramic composite materials. The fibre reinforcement is necessary to provide the required ductility. In this work, the behaviour of pure SiC under irradiation by He implantation is studied. Samples are investigated by means of the extended X-ray absorption fine structure (EXAFS) spectroscopy, performed at the Si K-edge. The Fourier transforms of the EXAFS data indicate a decrease of the Si–Si bond related shells around the absorbing Si. The possible damage features are discussed and the three most probable ones for the irradiation conditions are selected for future modelling work.

1. Introduction

1.1. Project background

The high temperature materials Project deals with potential structural materials for new types of nuclear reactors. The so called very high temperature reactor (VHTR) is developed in the frame of the international Generation IV initiative [1]. The idea is to directly use the heat of the gas cooled system for hydrogen production (for example by using a thermochemical processes like the iodine–sulphur (I–S) cycle) and/or to drive a He-gas turbine with a much increased efficiency. For efficient operation the I–S process requires temperatures above 1175 K. This implies gas-temperatures of more than 1225 K. Some of the core materials have to withstand 1275 K for 60 years under irradiation. The materials being investigated at PSI are (Si)C_f/(Si)C composites, oxide dispersion strengthened (ODS) steels such as PM2000, and intermetallics such as TiAl.

Fibre reinforced ceramics are promising candidates for high temperature materials. Joining the very good ability of SiC to endure high temperature and irradiation conditions with the ductility introduced by the reinforcement, makes SiC/SiC the ideal material for reactor internals. SiC as a basis for the composite is a well-known material, which has already been widely investigated towards its behaviour at high temperature and under irradiation. In the non-nuclear field, SiC is widely investigated and used for aeronautics and space applications [2], in the nuclear field, it is mainly investigated for fusion-applications [3,4].

1.2. The Material – SiC and possible damage modes

The material being investigated in this study is an α-SiC with hexagonal structure (Space Group P63mc, No. 186) [5]. It is present as a mixture of its 4H and 6H form (see Fig. 1, and Ref. [6,7]). These structures display the stacking sequences *abcb* and *abcacb*, respectively, and alternating hexagonally and cubically coordinated bilayers. For the composition see the sample description in the experimental Section 2.1.

1.2.1. Behaviour under irradiation

This study deals with the elemental irradiation behaviour of bulk SiC. Although in the nuclear field the material would be applied as basis for composite materials (e.g. SiC – fibre reinforced SiC matrix or C matrix), researching bulk SiC is interesting to understand the damage arising from irradiation. For the understanding of SiC composites, with much more complex damage modes, and for neutron irradiation damage, see for example Ref. [8].

In bulk SiC different damage modes are possible. These are the introduction of cavities within the crystal originating from the incoming ions, from which the energy loss along their travelling track could form channels. Another possibility for a cavity formation, are the He clusters, which grow with increasing He fraction being implanted into the material (resulting in platelets finally). The third possible damage mode is the displacement of single

* Corresponding author. Tel./fax: +41 56 310 2245.
E-mail address: manuel.pouchon@psi.ch (M.A. Pouchon).

0022-3115/$ - see front matter © 2008 Elsevier B.V. All rights reserved.
doi:10.1016/j.jnucmat.2008.12.017

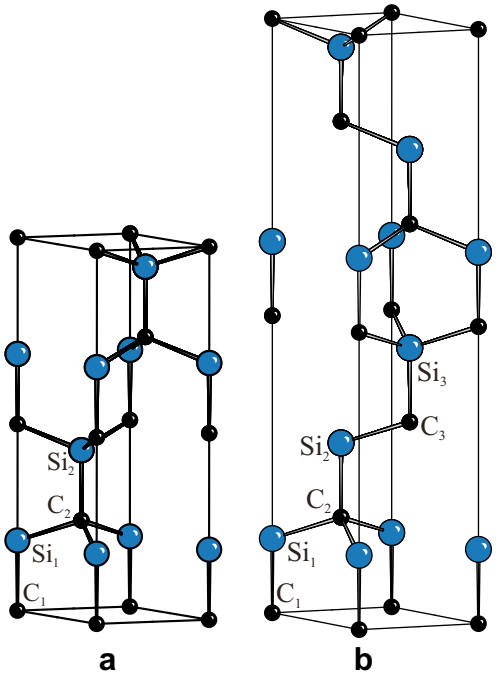

Fig. 1. (a) SiC 4H-Structure, with a, b = 3.073 Å, c = 10.053 Å (b) SiC 6H-Structure, with a, b = 3.073 Å, c = 15.079 Å.

atoms, and potentially their clustering. Finally the amorphisation and the depletion to pure Si are also possible damages being introduced into the material.

1.2.2. Formation of cavities

The formation of ion tracks during irradiation is mainly observed for heavy ion implantations into ceramics. Ref. [9] shows for example a 173 MeV ^{129}Xe implantation to a fluence of 2×10^{12} cm^{-2} into epitaxial Y–Ba–Cu–O films. Here the tracks are well visible on a high resolution TEM photograph.

The formation of nano-platelets is shown experimentally (TEM) for the actually investigated material here, see the corresponding scheme in Fig. 6a and the micrograph in Fig. 6b (see also Ref. [5]). With the irradiation damage being introduced by a He implantation, and the therefore very high appm/dpa ratio, the platelet formation is also seen as a very probable damage mode here (appm is atom part per million, which here describes the He concentration in the matrix, dpa are the displacement per atom).

1.2.3. Shifting of single atoms

The thesis work [10] represents a good basis for the shifting of single atoms, the creation of point defects. These can be vacancies, interstitials and in the case of compound materials, like SiC, antisites. The defects are addressed by *ab-initio* modelling and the resulting simulated phonon spectra are compared to experimental ones. In order to evaluate this damage mode for the samples being investigated here, atomistic *ab-initio* modelling for the predominant 6H structure is foreseen. The full structure with the exact shifting of all atoms is necessary to perform the *ab-initio* multiple scattering calculations necessary to receive the corresponding EXAFS spectra.

1.2.4. Change of structure due to radiation

In [11] the structural change of 6H–SiC due to electron irradiation is directly observed by transmission electron microscopy (TEM). At low temperature, amorphisation is observed, during irradiation at higher temperatures (~525 K), the formation of crystalline silicium is formed due to depletation of the carbon and high damage recovery rate at this elevated temperature. To amorphize the structure at 105 K, about 4 dpa are necessary, at room temperature, 100 dpa. In [12] 6H SiC is irradiated at 77 K, and in the radial distribution function, a reduction of the peaks, associated with the Si-atoms, is measured with increasing radiation. The higher Si-shells get even more reduced. This is interpreted as a breakdown of the tetrahedral network, while the tetrahedrals themselves stay intact.

2. Experimental

2.1. Sample preparation and implantation

Polished sheets of 0.33–0.36 mm thickness of hot pressed silicon carbide (SiC-HD, density: 3.2 g cm^{-3}, purity: ⩾ 98.5%) were supplied by Elektroschmelzwerk Kempten. X-ray analysis showed a composition of 80% 6H–SiC, 18% 4H–SiC and small amounts of 3C–SiC (β-SiC), 15R–SiC, and free carbon. The samples were irradiated on the Jülich compact cyclotron with 0–24.7 MeV He ions up to 2500 appm He concentration, the energy range is achieved by the use of a degrader wheel, with a variety of foils with different thickness, in this configuration the maximal implantation depth into the sample was roughly 200 μm. The samples were implanted at ambient temperature (325–375 K) and under vacuum (~10^{-3} Pa). For a more detailed description of the sample preparation and the accelerator facility see [5]. The implanted He concentration and the corresponding displacement dose are specified in Table 1. The samples were not annealed.

2.2. EXAFS and EXAFS evaluation

The EXAFS spectra were measured at the LUCIA-Beamline of the Swiss Light Source / PSI [13]. The characteristics are as follows: the energy is from 0.8 to 8 keV, the photon flux is 2×10^{12} s^{-1}, the beam size is 1.2 × 1 μm. The measurements were performed at the Si K-edge (1839 eV) in fluorescence mode with an incoming X-ray being perpendicular to the surface and the detector having a grazing angle of 12° from the surface as illustrated in Fig. 2. The samples were non-irradiated reference silicon carbide and irradiated silicon carbide with different implantation doses (see Table 1). Additionally some total electron yield spectra were taken (not shown in this paper). A repeating sequence of measurements

Table 1
Irradiation conditions: samples with corresponding implantation dose in appm (atom parts per million) and displacement damage in dpa (displacements per atom). *Results from the radial distribution function (RDF):* height and area of three selected peaks, at 1.75 Å corresponding to a Si–C bond, 2.91 Å corresponding to a Si–Si bond, and 6.01 Å also corresponding to a Si–Si bond. The results for the Reference and T2 represent an average from two measures. The Sample T8 is greyed out, because the results seem unrealistic (see text). The peak area was measured by fitting of three split Gaussian functions into the two first peaks, and one split Gaussian function into the third peak (split Gaussian: different 'half-width at half-maximum' before and after the 'median').

Sample	He concentration (appm)	Damage (dpa)	RDF peak height/area ($Å^{-4}$)/($Å^{-3}$) at R:		
			1.75 Å	2.91 Å	6.01 Å
Reference	–	–	3.76/ 2.22	6.77/ 3.41	2.41/ 1.47
T3	194	0.012	3.78/ 2.20	5.94/ 2.88	1.90/ 1.19
T7	600	0.036	3.35/ 2.61	5.95/ 3.15	1.84/ 0.98
T8	1500	0.090	3.33/ 2.36	6.84/ 3.94	2.29/ 1.33
T2	2451	0.147	3.25/ 2.42	4.31/ 2.71	1.07/ 0.57

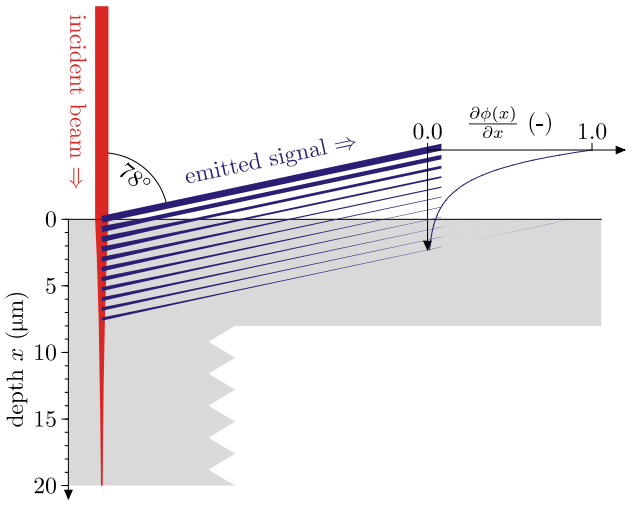

Fig. 2. XAFS analytical scheme, with a perpendicular incoming beam absorbing through the material, the fluorescence X-rays and their detection within a 12° angle from the surface. Seventy five% of the signal is issued from the material below 500 nm from the surface. The XAFS results are therefore assumed to reflect the bulk properties of SiC.

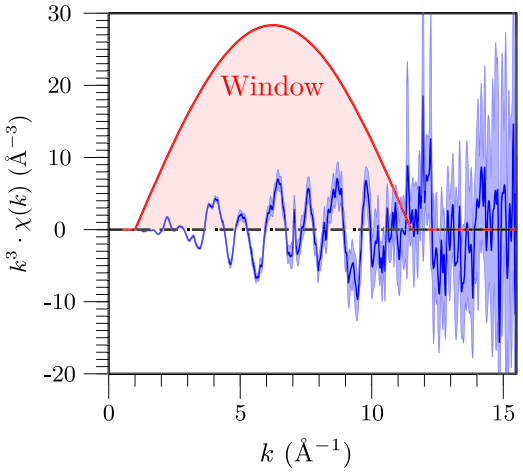

Fig. 3. Experimental EXAFS result for the reference sample. The high quality of the data is provided by selecting a sine window $\omega(k)$ from $k = 2.0$–10.5 Å^{-1} for the Fourier transformation. The centre-line is the averaged data surrounded by an area and two thin lines representing the standard deviation of the data.

was programmed, where all samples were measured during each execution. Seven sequences could be measured, allowing a good statistics.

The spectra were evaluated using the ATHENA code [14]. For the Fourier transformation a sine window from 2.0 to 10.5 Å^{-1} was chosen. Fig. 3 shows the EXAFS spectra taken from the reference sample. The graph shows the window applied for all Fourier transformations. The spectra consists of a middle line, being the average of 7 measurements, surrounded by an area limited by thin lines, representing the corresponding standard deviation. This should give an idea about the data quality, and also justify the high k range being usable in the evaluations. For the irradiated samples, only four spectra were taken for each, avoiding the noisiest ones.

The influence of the self absorption is verified using the booth algorithms [15], which can be addressed directly within the ATHENA code. For the reference material, the only effect showing due to this correction is a doubling of the peak intensity. When forming the ratio of the two signals, a constant value of 2.0 results throughout the whole spectra, with some variations where the absolute signal value is small (larger error). As in frame of this study, only the relative change of the signal is of interest, the self absorption correction is not conducted for the rest of the measurements.

In order to evaluate the radial distribution functions, some selected peaks are fitted and evaluated toward their height and area. As the peak shape does not correspond to any classical distribution functions, the first two peaks were fitted by three split Gaussians each, and the third peak with a single split Gaussian. The results of both, the peak height and the peak areas are reported numerically in Table 1. The more sophisticated peak simulation using *ab-initio* multiple scattering calculations (using the program FEFF [16]) is going to be performed in a later stage, giving more insight into the possible damage mode.

3. Results and discussion

In order to describe the XAS signal pathway, a scheme including absorption excitation and reemission is suggested in Fig. 2. Most of the information (83%) is yielded from a shallow layer of only 3 µm below the surface and about 25% from the first 500 nm. Nevertheless, 75% of the signal is generated by the material deeper than 500 nm below the surface. Assuming that this material has bulk properties, which are relevant for the project, this signal fraction represents relevant information. Concentrating on the Si K edge data, and optimising the Fourier transformation analysis, the results focus on the change of the radial distribution function with irradiation. Fig. 4 shows the Fourier transforms of non-irradiated samples (Reference) up to irradiated samples with He implantation doses of 2451 appm (corresponding to a displacement damage of 0.147 displacements per atom dpa). For a full list of samples,

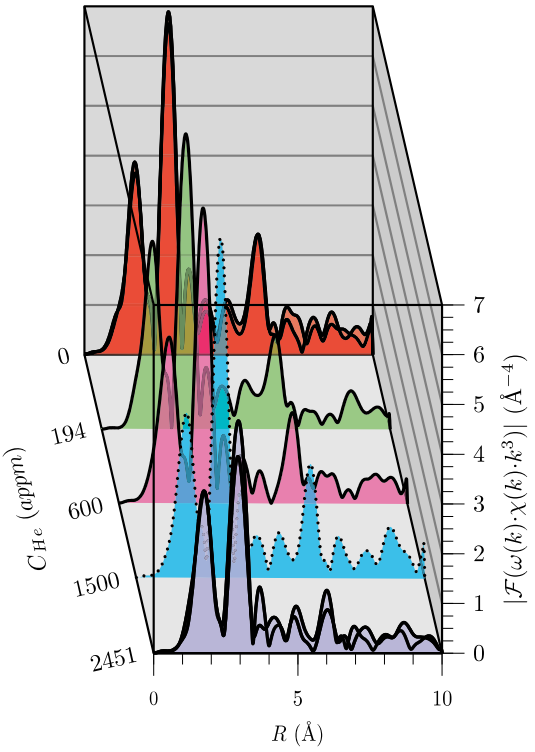

Fig. 4. Radial distribution functions (RDF) for all measured samples. The spectra are stacked diagonally to the left with the highest implantation dose $C_{He} = 2451$ appm in front, and the non-irradiated material in the very back. The fist peak remains almost unchanged; the second one clearly decreases with implantation dose (with the exception of 1500 appm). For a better understanding, the two first peaks plus the peak around 6 Å are extracted and represented separately in Fig. 5. For the reference and for the highest helium concentration, two samples were measured. Both RDFs if each are shown here, to demonstrate the comparability of the results.

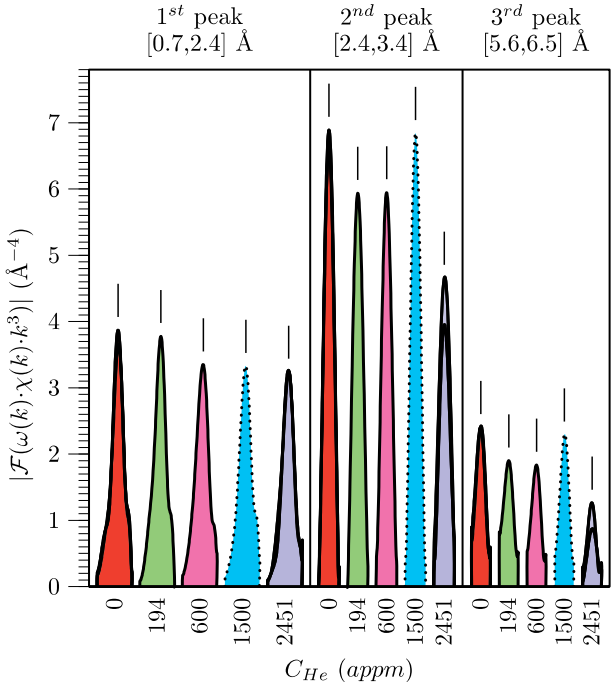

Fig. 5. Crop (from Fig. 4) of the first, second and third peaks as a function of the implantation dose. The fist peak (left, from 0.7 to 2.4 Å) remains almost constant with a small but consistent decrease with implantation dose. The second peak (middle, from 2.4 to 3.4 Å) shows a clear and important decrease with implantation dose, except for the measurements on sample T8 with a He concentration of C_{He} = 1500 appm. The same also applies for the third peak (right, from 5.6 to 6.5 Å). The marks above the peaks note the *R* positions at 1.75, 2.91 and 6.01 Å for the first, second and third peak, respectively. The sample T8 is drawn with a dotted line, because an uncontrolled irradiation parameter seems probable (see text).

implanted He concentration and displacement damage see Table 1. In the Fourier transformations of the EXAFS spectra, corresponding to a radial distribution function (RDF) three peaks are investigated more closely here. These correspond to the first and second shell being the first Si–C bond (at 1.88 Å) and Si–Si bond (at 3.08 Å) around the absorbing Si atom, and to a Si–Si bond at 6.01 Å (see Fig. 1 for an understanding of the structure). All three peaks are isolated and represented as a function of the implantation dose in Fig. 5. The peak heights are noted in Table 1 together with the corresponding peak area. The first peak at 1.75 Å on the left of Fig. 5 shows a minor but steady decrease as a function of the irradiation dose. For 194 appm the peak height remains constant (increase by 0.7%), then it decreases by 10.8%, 11.3% and 13.4% for 600, 1500 and 2451 appm, respectively. The corresponding area also remains constant (decrease by 0.6%) and then increases by 17.6%, 6.6% and 9.0%. This means a broadening of this peak and could be explained by a distortion of the corresponding C atoms. The second peak at 2.91 Å shows a major decrease in peak height, but has an inconsistence for the sample being implanted to 1500 appm. The decrease is as follows, 12.2%, 12.0% and 36.4% for 194, 600 and 2451 appm respectively and for 1500 appm the amplitude slightly increases by 1.1%. The corresponding areas also decrease by 15.7%, 7.8% and 20.6%, and at 1500 appm increase by 15.5%. Here both, the peak height and the peak area show the same behaviour. This could signify a loss of atoms at this distance, being displaced to another location, and therefore a reduction of the coordination number. The third peak at 6.01 Å shows a very similar behaviour to the second one. The amplitude decreases by 21.2%, 23.7% and 55.8% for 194, 600 and 2451 appm, respectively, and the area also decreases by 19.5%, 33.4% and 61.8%. As before, the sample irradiated to 1500 appm, shows an inconsistent behaviour, only reducing its peak height by 5.0% and the peak area by 9.8%. If neglecting this one sample (T8), the second and third peaks seem to show the same important radiation effect. In both cases the de-

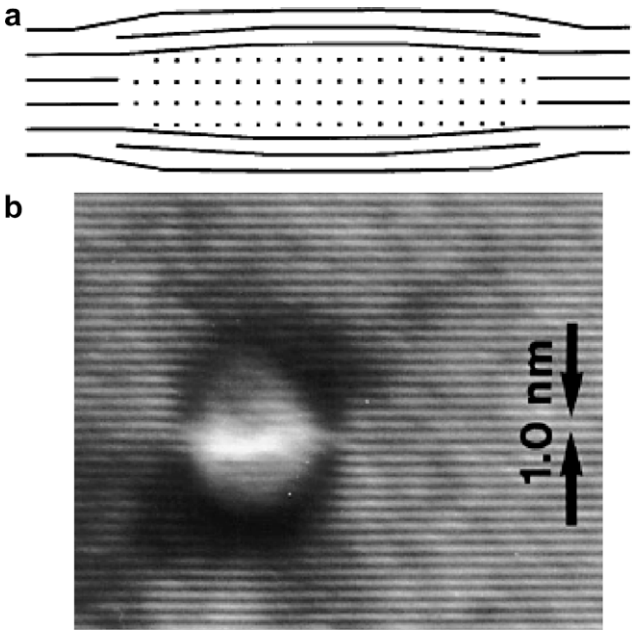

Fig. 6. (a) Scheme of a heliusm filled crack (platelet) taken from [5] and (b) a TEM picture of a platelet with the electron beam in [$2\bar{1}\bar{1}0$] direction. The platelet lays in a habit plane of [0001] in the coordinate system of the hexagonal Bravai's cell.

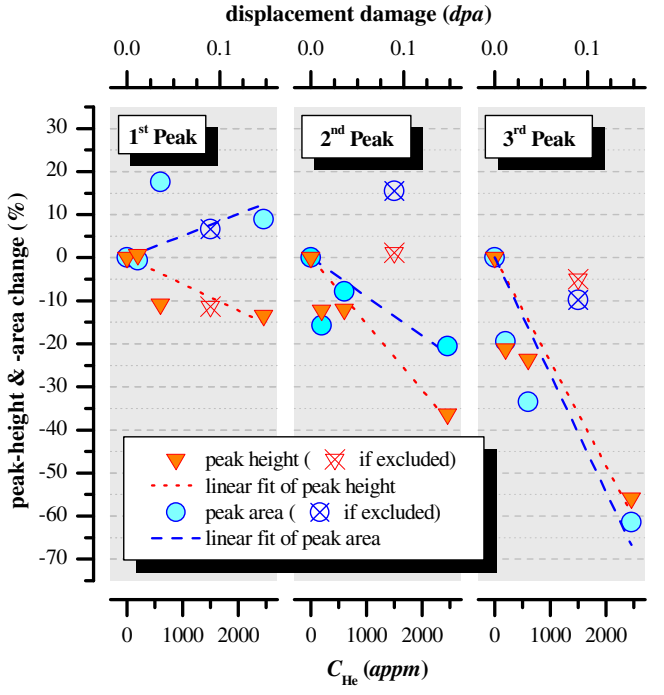

Fig. 7. Changes of heights and areas for the first, second and third peaks described in Fig. 5 and listed with the corresponding values in Table 1. Linear trend-lines are added for both, the peak height and peak areas. The sample irradiated to 1500 appm is excluded from these trend-lines and plotted with different symbols in the graph (see text explanation). Interesting is the different behaviour of the Si–C binding related first peak compared to the Si–Si binding related second and third peaks. In the first case the height decreases, but the area remains (or even increases), which is a hint for a distortion of the corresponding C atoms, whereas in latter cases both, the height and area decrease in about the same manner, which is a hint for displaced atoms.

crease in coordination number is much more important, than what the fraction of atoms being displaced (0.147 dpa) would allow. The inconsistent results from the sample T8 lead to the assumption, that at the measurement point, the beam might not have reached the sample. The results from this sample are fully reported, but no conclusion should be drawn from it. An overview of all these peak changes as a function of irradiation is represented in Fig. 7.

The findings are very similar to the results obtained in [12], where a break of the tetrahedral networks is seen as reason for the change in the radial distribution function. However, the irradiation conditions in the present experiment are quite different; the irradiation temperature is 325–375 K instead of 77 K. According to [11] this would require a more than two orders of magnitude higher displacement dose, to get full amorphisation, and probably the same ratio applies to the detection of such a network breakup. The results however indicate a similar effect, and the tetrahedral breakup should also be considered as a damage mode.

4. Conclusions

Composite materials of silicon carbide are investigated as possible structural material for the future generation of nuclear reactors. Bulk silicon carbide samples, mainly composed of the 6 H- and 4H–SiC structures, are therefore investigated regarding their radiation resistance. A helium ion beam with an energy distribution ranging from 0 to 24 MeV was used to implant the samples to different dopant doses and hence to different displacement damages. The highest dose is 2451 appm, corresponding to the displacement damage of 0.147 dpa. The samples are then investigated by means of the extended X-ray absorption spectroscopy (EXAFS). A clear difference in the EXAFS spectra can be observed with increasing displacement dose. The Fourier transform shows clearly a strong decrease of the coordination number in the Si–Si peaks at 2.91 and 6.01 Å, corresponding to the next neighbouring and a further shell of silicon atoms. The pure displacement cannot explain the important decrease in coordination number in these shells. Therefore, the authors suggest the modelling of three damage modes. These are the pure point defects, the breakup of the tetrahedral network and the formation of He platelets.

Acknowledgements

The work was performed within the Swiss Generation IV Program; it was partially financed by the EU-projects F-BRIDGE and EXTREMAT.

References

[1] The Generation IV International Forum, OECD Nuclear Energy Agency, <www.gen-4.org/>.
[2] D. Gay, S.V. Hoa, S.W. Tsai, Composite Materials, Design and Applications, CRC Press, 2003.
[3] Y. Katoh, L.L. Snead, C.H. Henager Jr., A. Hasegawa, A. Kohyama, B. Riccardi, H. Hegeman, J. Nucl. Mater. 367–370 (2007) 659.
[4] R.T. Bhatt, S.R. Choi, L.M. Cosgriff, D.S. Fox, K.N. Lee, Mater. Sci. Eng. A 476 (2008) 8.
[5] J. Chen, P. Jung, H. Trinkaus, Phys. Rev. Lett. 82 (1999) 2709.
[6] N.W. Thibault, Am. Mineral. 29 (1944) 327.
[7] J.A. Powell, P. Pirouz, W.J. Choyke, 'Growth and characterisation of silicon carbide polytypes for electronic applications', Semiconductor Interfaces, Microstructures and Devices, Institute of Physics Publishing (1993) 257.
[8] G. Newsome, L.L. Snead, T. Hinoki, Y. Katoh, D. Peters, J. Nucl. Mater. 371 (2007) 76.
[9] B. Hensel, B. Roas, S. Henke, R. Hopfengärtner, M. Lippert, J.P. Ströbel, M. Vildić, G. Saemann-Ischenko, S. Klaumünzer, Phys. Rev. B: Condens. Matter 42 (1990) 4135.
[10] A. Mattausch, 'Ab initio-Theory of Point Defects and Defect Complexes in SiC', PhD thesis #1789, Erlangen 2005, <www.opus.ub.uni-erlangen.de/opus/volltexte/2005/178/>.
[11] I. Bae, M. Ishimaru, Y. Hirotsu, Nucl. Instrum. Methods. Phys. Res., Sect. B 250 (2006) 315.
[12] W. Bolse, Nucl. Instrum. Methods. Phys. Res., Sect. B 148 (1999) 83.
[13] A.-M. Flank, G. Cauchon, P. Lagarde, S. Bac, M. Janousch, R. Wetter, J.-M. Dubuisson, M. Idir, F. Langlois, T. Moreno, D. Vantelon, Nucl. Instrum. Methods Phys. Res., Sect. B 246 (2006) 269.
[14] B. Ravel, M. Newville, J. Synchr. Rad. 12 (2005) 537.
[15] C.H. Booth, F. Bridges, Phys. Scr. T115 (2005) 202.
[16] A.L. Ankudinov, C.E. Bouldin, J.J. Rehr, J. Sims, H. Hung, Phys. Rev. B: Condens. Matter 65 (2002) 104107.